



Experimental Design and Implementation of IT2FL-controlled BLDCM Based on LabVIEW™

Hayder Yousif Abed, Abdulrahim Thiab Humod, Amjad J. Humaidi, Ayad Q. Al-Dujaili

Abstract: This article presents design and implementation of Interval Type-2 Fuzzy Logic Controller (IT2FLC) for speed control of brushless DC motor (BLDCM) based on LabVIEW package. For the purpose of comparison, the performance of IT2FLC is compared to Type-1 FL controller (TIFLC). For fair comparison, both schemes of FL controllers are set with the same number of membership functions and input-output gain values. The robustness characteristics of both FL controllers are assessed in terms of dynamic performance and load rejection capability. The design of IT2FLC and TIFLC are made and implemented within LabVIEW environment and the effectiveness of controllers are verified experimentally. The experimental results showed that IT2FL controller gives better robustness under load variation than conventional TIFL controller.

Keywords : Type-1 FL controller, Interval type-2 FL controller, BLDCM, Speed control

I. INTRODUCTION

Brushless DC motors (BLDCMs) are used in several fields and have many applications, such as in industrial automation, electric vehicles and aerospace computers. BLDCMs exhibit several advantages over brushed DC motors. In particular, they require lower maintenance due to the disposal of the commutator, have longer operating life due to the lack of friction and electrical losses and achieve higher power density; these characteristics make them ideal candidates for applications that require high electromagnetic torque-to-weight ratio [1]. Compared with brushed DC motors and induction machines, BLDCMs have lower inertia, enabling faster dynamic response to reference commands. They are also more efficient due to the presence of permanent magnets, which can perform with virtually zero rotor losses [1].

Recently, various modern control solutions are proposed for the speed control of different structures of high performance motors [2-5]. The intelligent control of BLDC motors has elicited the attention of many researchers. A review of the most relevant studies is presented hereafter.

R. Arulmozhiyal and R. Kandiban compared a conventional proportional–integral–derivative (PID) controller and a fuzzy PID controller for speed control of BLDC motors. The results are firstly simulated based on MATLAB/SIMULINK and then verified experimentally. The simulated and practical results showed that the fuzzy PID controller outperformed the conventional PID controller [6]. E. Blessy and M. Murugan analysed a BLDC motor model and designed FL controller to improve the dynamic performance of speed control. They compared the fuzzy logic (FL), proportional, proportional–integral–derivative (PID) controllers to evaluate the impact of each controller on speed dynamic performance [7]. Mohammed A. Shamseldin and Adel A. EL-Samahy presented three different robust controllers for the speed regulation and tracking control of high-performance BLDC motors. These controllers are conventional PID, genetic-based PID and self-tuning fuzzy PID controllers. Genetic optimization and self-tuning intend to find the best gains of PID controllers in terms of transient and steady-state characteristics. The work showed that the self-tuning fuzzy PID controller outperformed the other control techniques [8]. P. Hari Krishnan and M. Arjun developed an adaptive FL PID controller to control the speed of a BLDC motor. They compared the fuzzy PID controller and the adaptive fuzzy PID controller. The simulation results based on MATLAB/SIMULINK showed that the adaptive fuzzy PID controller exhibited better performance than the fuzzy PID controller [9]. Akhila M. and Ratnan P. introduced an adaptive neuro-based fuzzy (ANFIS) controller for electric vehicles based on BLDC motors. They adopted a regenerative braking strategy to maintain the vehicle's stability and recover energy, thereby reducing air pollution and achieving optimum energy utilisation. The simulation in MATLAB showed that the ANFIS-based controller could rapidly reach the target and overcome the complexity of the problem [10]. Shu Xiong et al. developed a radial basis function (RBF) neural network with a PID controller to overcome the response lag, low precision and instability problems due to the use of the classical PID controller in the speed control of BLDC motors.

Manuscript published on November 30, 2019.

* Correspondence Author

Hayder Yousif Abed*, PhD student, Department of Electrical and Electronic Engineering, University of Technology, Iraq.

Amjad J. Humaidi, Deputy Dean, Department of Control and System Engineering, University of Technology, Iraq.

Abdulrahim Thiab humod, Asst. Professor, Department of Electrical and Electronic Engineering, University of Technology, Iraq.

Ayad Q. Al-Dujaili, PhD student, Department of Electrical and Electronic Engineering, University of Technology, Iraq.

© The Authors. Published by Blue Eyes Intelligence Engineering and Sciences Publication (BEIESP). This is an open access article under the CC-BY-NC-ND license <http://creativecommons.org/licenses/by-nc-nd/4.0/>

The simulation results showed that the proposed intelligent controller could effectively improve the performance of the controlled system and provide faster response than the traditional PID controller [11].

Muhammed A. Ibrahim et al presented an optimal speed control design of Brushless DC motor based on genetic algorithm (GA). The optimization method is employed to find optimal values of Proportional–Integral–Derivative (PID) parameters in terms of better dynamic performance [12]. N. N. Baharudin and S. M. Ayob utilized hybrid conventional and intelligent controller to cope with the drawback of both controllers. The conventional controller is represented by linear controllers such as PI, PID and PD controller, while the intelligent controller is designed based on FL control [13].

One main issue in control of BLDC motor is how to design a controller such as to obtain high dynamic performance and to cope with system uncertainty and load disturbance. The conventional controller lacks the ability to give satisfactory responses under parameter variation and load application. Therefore, FL controller is proposed to replace the classical controllers to solve the degrade in system performance due to uncertainty in system parameters. Two schemes of FL controllers, represented by Type-1 and IT2FL controller, are presented in this work. The main contribution of the present work can be summarized as:

1. Design and implementation of IT2FLC and T1FLC for the speed control of BLDCMs.
2. Performance comparison between IT2FLC and T1FLC in terms of transient and disturbance rejection capabilities.

II. DYNAMIC MODEL OF BLDCM

BLDCM is a three-phase, star-connected, four-pole and trapezoidal back electromotive force (EMF) motor with a three-phase inverter. Fig.1 shows the basic block diagram for the speed control of BLDCM.

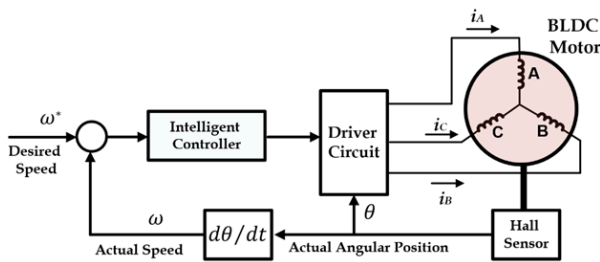


Fig. 1. Basic block diagram of the sensor-less drive of BLDCM

The voltage equations for BLDCM can be described by the following set of equations [10]:

$$v_a = R_{as}i_a + L_{aa}\frac{d}{dt}(i_a) + L_{ab}\frac{d}{dt}(i_b) + L_{ac}\frac{d}{dt}(i_c) + e_{as} \quad (1)$$

$$v_b = R_{bs}i_b + L_{ba}\frac{d}{dt}(i_a) + L_{bb}\frac{d}{dt}(i_b) + L_{bc}\frac{d}{dt}(i_c) + e_{bs} \quad (2)$$

$$v_c = R_{cs}i_c + L_{ca}\frac{d}{dt}(i_a) + L_{cb}\frac{d}{dt}(i_b) + L_{cc}\frac{d}{dt}(i_c) + e_{cs} \quad (3)$$

where v_a , v_b and v_c are the stator phase voltages; R_a , R_b and R_c are the phase resistances of the stator; i_a , i_b and i_c are the currents of the stator phases; L_{aa} , L_{bb} and L_{cc} are the

self-inductances of the stator windings; L_{ab} , L_{bc} , L_{ba} , L_{ac} , L_{ca} and L_{cb} are the mutual inductances amongst the stator windings and E_a , E_b and E_c are the back EMFs of the three phase stators [10]. Given the symmetric structure and equal resistances of the three stator windings, we derive

$$L_{aa} = L_{bb} = L_{cc} = L \quad (4)$$

$$L_{ac} = L_{ab} = L_{ba} = L_{bc} = L_{ca} = L_{cb} = M \quad (5)$$

where L is the self-inductance of the stator and M is the mutual inductance. L and M are independent of the rotor position. The three-phase star winding motor can be expressed as follows:

$$i_a + i_b + i_c = 0 \quad (6)$$

$$Mi_a + Mi_b + Mi_c = 0 \quad (7)$$

The instantaneous induced EMFs can be described by

$$e_{ats} = f_{as}(\theta_r) \lambda_p \omega_m \quad (8)$$

$$e_{bts} = f_{bs}(\theta_r) \lambda_p \omega_m \quad (9)$$

$$e_{cts} = f_{cs}(\theta_r) \lambda_p \omega_m \quad (10)$$

where ω_m is the rotor angular speed and θ_r is the rotor position. The complete model for BLDCM can be written in matrix form using equations. (1), (2) and (3) as follows [15]:

$$\begin{pmatrix} v_a \\ v_b \\ v_c \end{pmatrix} = \begin{pmatrix} R_s & 0 & 0 \\ 0 & R_s & 0 \\ 0 & 0 & R_s \end{pmatrix} \begin{pmatrix} i_a \\ i_b \\ i_c \end{pmatrix} + \begin{pmatrix} L_{aa} & L_{ab} & L_{ac} \\ L_{ba} & L_{bb} & L_{bc} \\ L_{ca} & L_{cb} & L_{cc} \end{pmatrix} \frac{d}{dt} \begin{pmatrix} i_a \\ i_b \\ i_c \end{pmatrix} + \begin{pmatrix} e_{as} \\ e_{bs} \\ e_{cs} \end{pmatrix} \quad (11)$$

All phase resistances are equal and can be designated by (R) because a balanced three-phase motor is considered. Therefore, equation (11) can be written as

$$\begin{pmatrix} v_a \\ v_b \\ v_c \end{pmatrix} = \begin{pmatrix} R & 0 & 0 \\ 0 & R & 0 \\ 0 & 0 & R \end{pmatrix} \begin{pmatrix} i_a \\ i_b \\ i_c \end{pmatrix} + \begin{pmatrix} L-M & 0 & 0 \\ 0 & L-M & 0 \\ 0 & 0 & L-M \end{pmatrix} \frac{d}{dt} \begin{pmatrix} i_a \\ i_b \\ i_c \end{pmatrix} + \begin{pmatrix} e_a \\ e_b \\ e_c \end{pmatrix} \quad (12)$$

where functions $f_{as}(\theta_r)$, $f_{bs}(\theta_r)$ and $f_{cs}(\theta_r)$ have the same shape as e_{ats} , e_{bts} and e_{cts} with a maximum magnitude of ± 1 . In addition, the induced EMFs have rounded edges rather than sharp corners as observed in the trapezoidal functions. This condition is attributed to the time derivative of the flux linkages. The flux density functions are smooth without sudden edges because the flux linkages are fringing and continuous functions. The expression for electromagnetic torque can be written as

$$T_e = (e_a i_a + e_b i_b + e_c i_c) / \omega \quad (13)$$

$$E_p = \lambda_p \omega_m \quad (14)$$

The developed torque, which is used to overcome the mechanical rotation and load torque, is expressed as

$$T_e = J \frac{d\omega}{dt} + B_f \omega_m + T_L \quad (15)$$

III. T1FLC AND TYPE-2 FLC (T2FLC)

The FLC design requires selecting membership functions (MFs). The selected MFs should cover the entire universe of discourse (UOD). They should also not overlap with one another to avoid any form of discontinuity with respect to minor changes in input [16]. T2FLC consists of a set of MFs that operate with 3D uncertainties. By contrast, the MFs of type-1 fuzzy sets operate with only two dimensions.

The fuzzy sets of MFs are shown in Fig. 2. These fuzzy sets are capable of modelling and handling uncertainties, nonlinearities and linguistic variables related to the input and output of FLCs by simulating them and reducing their effectiveness. T1FLC fuzzy sets supplement classical fuzzy sets, clearly indicating the preferences of IT2FLC [17].

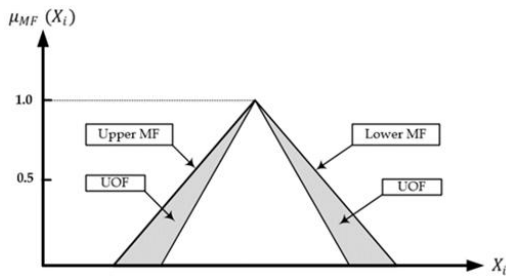


Fig. 2. MF structure of IT2FLC

The mathematical equation for a system is required to control practical systems on the basis of the traditional control design. Most system equations that describe system dynamics are differential equations associated with either continuous or discrete time systems. Most physical systems are complex and nonlinear in reality. An accurate nonlinear model is difficult to develop for most systems. Although a relatively exact model can be derived, designing a controller that can achieve the required dynamics is too complex, particularly for traditional control designs that impose certain assumptions on a system (e.g. system linearity). The advantages of T2FLCs over T1FLCs can be summarised as follows [18]-[21]:

- T2FLCs are more robust than T1FLCs because they can work under a wider range of operating conditions than T1FLCs. In addition, T2FLCs can deal with noise and load changes in a plant.
- The sets and MFs of T2FLCs are fuzzy. Moreover, the uncertainty can handle and model numerical uncertainties, nonlinearities and linguistic variables that are accompanied by the input and output of UOD for FLCs.
- The uncertainty of type-2 fuzzy sets can adopt the same UOD as that of type-1 fuzzy sets but with a smaller number of labels.

The following definitions describe the basic mathematical concepts of T2FLCs [22].

Definition 1. If \tilde{A} denotes type 2 fuzzy sets which are characterised by MF $\mu_{\tilde{A}}(x, u)$, where $x \in X$, X is the universe of discourse (UOD), and $u \in J_x \subseteq [0, 1]$, then

$$\tilde{A} = \{(x, u), \mu_{\tilde{A}}(x, u) | x \in X, u \in J_x \subseteq [0, 1]\} \quad (16)$$

$$\tilde{A} = \int_{x \in X} \int_{u \in J_x} \frac{\mu_{\tilde{A}}(x, u)}{(x, u)} J_x \subseteq [0, 1] \quad (17)$$

where $0 \leq \mu_{\tilde{A}}(x, u) \leq 1$. The equation can be expressed as where $\int \int$ represents the union over all admissible u and x .

Definition 2. A 2D system with axes u and $u_2(x, u)$ is known as the vertical slice of $u_2(x, u)$, which is represented as

$$\mu_{\tilde{A}}(x = x_1, u) = \mu_{\tilde{A}} = \int_{u \in J_x} \frac{\mu_{\tilde{A}}(x, u)}{(x, u)} J_{x_1} \subseteq [0, 1], \quad (18)$$

where $0 \leq f_{x_1}(u) \leq 1$ and $\mu_{\tilde{A}}(x)$ are defined as the secondary MF and secondary set, respectively. The primary MF of x_1 is designated by J_{x_1} and is the domain of the secondary MF, where $J_{x_1} \subseteq [0, 1]$ for all $x_1 \in X$.

Definition 3. The amplitude of the secondary MF is defined as the second degree, which is referred to as the secondary grade.

Definition 4. The bounded area of uncertainty for the type-2 fuzzy set \tilde{A} is called the footprint of uncertainty (FOU). FOU defines the union of all primary MFs. This union can be described as

$$FOU(\tilde{A}) = U_{x \in X} J_x \quad (19)$$

Definition 5. The upper and lower MFs of \tilde{A} are two type-1 fuzzy sets wherein the boundaries of $FOU(\tilde{A})$ for type-2 fuzzy set \tilde{A} are the lower and upper bounds of the type-1 fuzzy sets. The lower MF is described as $\underline{\mu}_{\tilde{A}}(x) x \in X$ and the upper MF is defined as $\overline{\mu}_{\tilde{A}}(x) x \in X$, indicating that

$$\overline{\mu}_{\tilde{A}}(x) = \overline{FOU}(\tilde{A}), \quad (20)$$

$$\underline{\mu}_{\tilde{A}}(x) = \underline{FOU}(\tilde{A}). \quad (21)$$

Lower and upper MFs frequently exist because the domain of the secondary MFs is limited within the range of [0, 1]. The structure of the interval type-2 FL membership of MFs with its secondary MFs is shown in Fig.3.

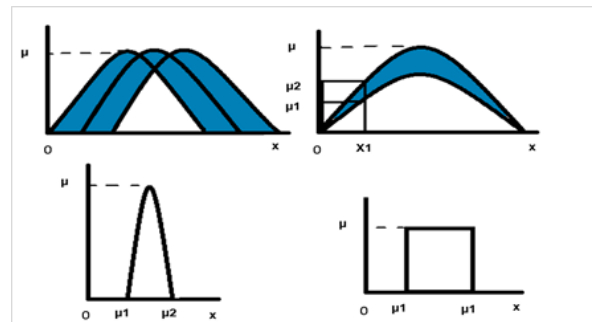


Fig. 3. Interval fuzzy type 2 MF structure with its secondary MFs

IV. EXPERIMENTAL RESULTS

Fig. 4 shows the hardware setup of the FL-controlled BLDCM. As indicated in the figure, the hardware assembly consists of a PC (Intel® Core™ i7 CPU 2.8 GHz), a BLDCM with the specifications listed in Table 1, a National Instruments data acquisition card (NI-PCI-6251) and a 24 V power supply with a 6.5 A single output.

The other accessories required for data interface are shielded channel connector block series devices for I/O connections (NI-BNC 2120), three oscilloscope AC/DC clamp current probe testers (CP-05A: 400 A, 200 KHz) and three high-voltage differential isolating probes (HT-8050: 50 MHz, 1300 V, 8 MΩ). The applied load involves a 12 V DC generator with a rheostat variable resistor (50 Ω) to provide variable loads. The experimental results are implemented using LabVIEW™ 2018.





(1) Personal computer. (2) DAQ Data acquisition card. (3) BNC connectors for I/O connections. (4) Power supply. (5) High voltage differential isolating probes. (6) Oscilloscope AC/DC clamp current probe. (7) Brushless DC motor. (8) DC generator. (9) Rheostat variable resistor.

Figure (4) Experimental Set-up of Controlled-based BLDCM

Table-I: Parameters of BLDC motor

Motor Parameters	Values
Number of poles	8
Number of phases	3
Stator Resistance	0.7 Ω
Stator Inductance	0.5×10^{-3} H
Rated power of motor	92 Watt
Rated speed of motor	3000 RPM
Rated torque of motor	0.22 N.m
Rotor inertia of motor	0.0075×10^{-3} Kg.m ²

Figs. 5 and 6 show the block diagrams of T1FLC and IT2FLC, respectively, synthesized using LabVIEW™ software. Fig. 7 depicts the mesh plot of the fuzzy surface within LabVIEW™. The surface defines the relation between control effort and the input of error e and change in error e. The knowledge base design will form the surface shown in the figure. This surface can accept the error and change in error until the equilibrium point at zero value. Notably, the software of FLCs is encoded and developed based on MATLAB's instructions for an m-file in LabVIEW™. The task of LabVIEW™ is to receive the output of an m-file, which represents the FLC, and direct it towards the external environment, where the BLDCM driver is located, under optimal interface conditions. In addition, LabVIEW™ receives speed information by utilising Hall sensors.

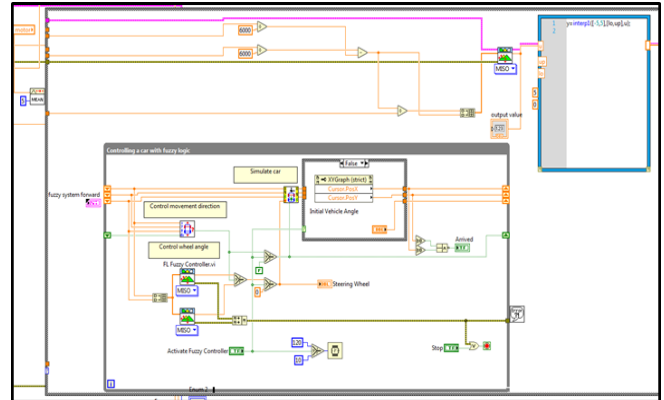


Fig. 5. Block diagram of Type1-FL controller within LabVIEW software

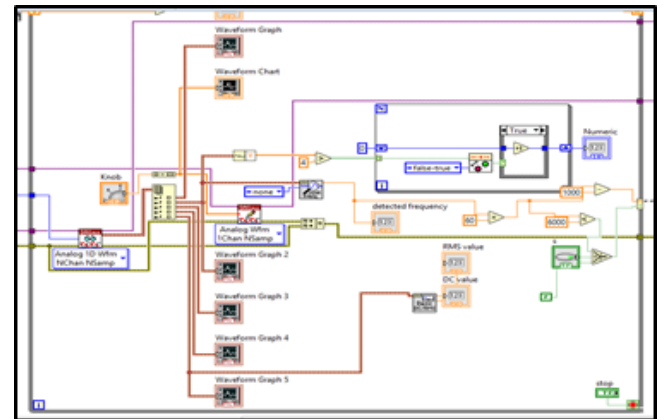


Fig. 6. Block diagram of IT2-FL controller within LabVIEW software

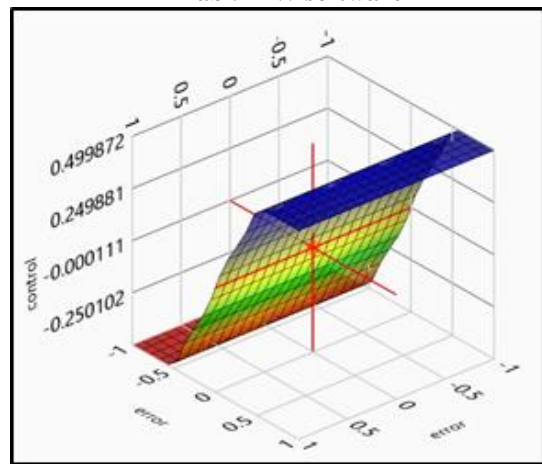


Fig. 7. The Type-1 FL control Surface which maps the relation of control effort, error, and change of error.

Fig. 8 shows the signals of a hall sensor motor rotor at a speed of 3000 RPM. The response of the hall sensor ranges from 5 V to -5 V. The control signal originating from the LabVIEW™ PC is applied to the BLDCM driver (SYS-BLD-120A). The control signal is entered into the driver as a pulse width modulation (PWM) waveform ranging from 0 V to 5 V. A controller (FAN7388), which is responsible for generating the appropriate control signals for the metal-oxide-semiconductor field-effect transistor gates, is located inside the motor driver. Fig. 9 shows the control signals in PWM waveform.

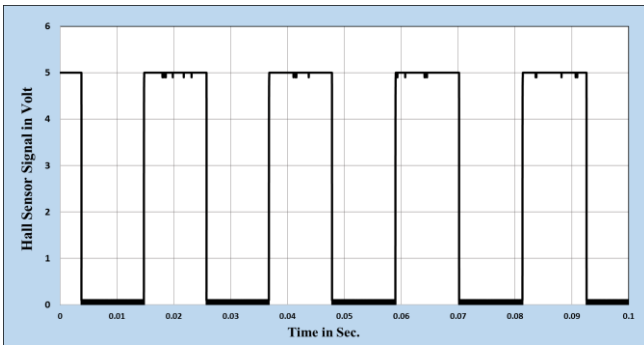


Fig. 8. The responses of Hall Sensor at speed 3000 RPM

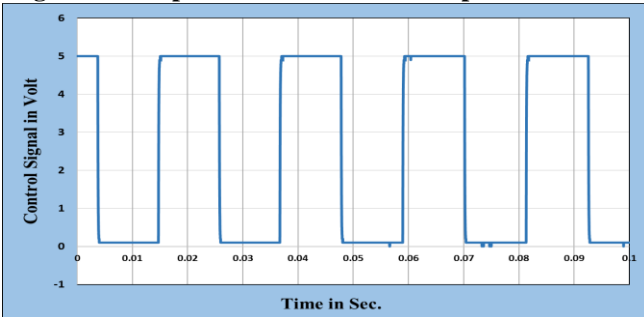


Fig. 9. The control signal in PWM waveform

Fig. 10 presents the speed response resulting from T1FLC. In this scenario, the reference speed is reduced from 3000 RPM to 2500 RPM at time 109 s and then allowed to return to 3000 RPM at time 171 s; a load of 0.2 N.m is applied during the time interval (264–334) s. The figure shows that a decline in speed of 212 RPM occurs upon load exertion. Moreover, T1FLC can regain the reference speed upon load release with a slight peak overshoot. However, T1FLC cannot follow the changed desired trajectory with zero error, and an error of 198 RPM is detected. The current signals of the BLDCM phases are shown in Fig.11. Fig. 12 illustrates the traces of line voltages at the BLDCM terminals.

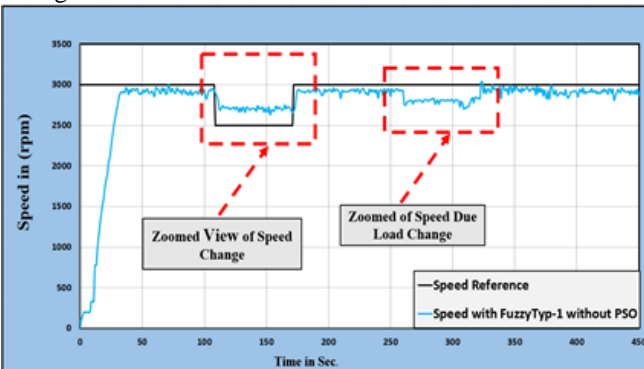


Fig. 10. The speed response of BLDC motor based on Type1-FL controller

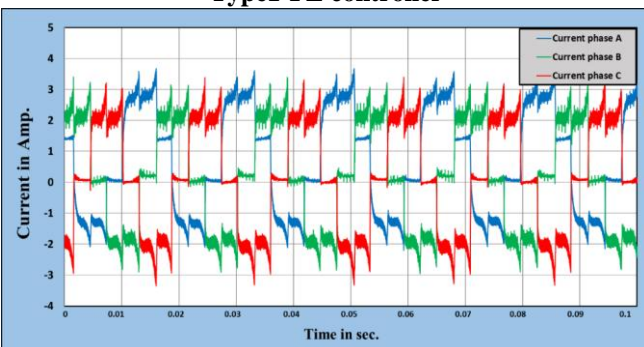


Fig. 11. The current signals of BLDC motor phases

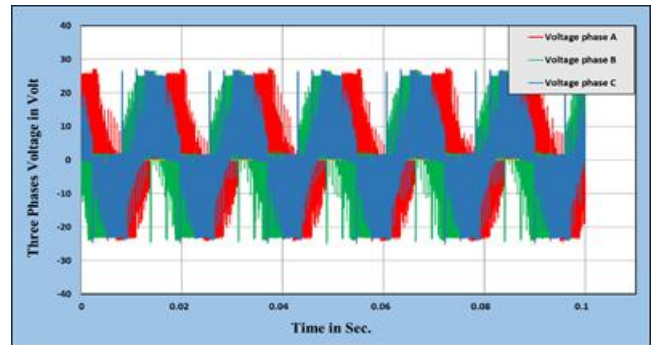


Fig. 12. Traces of line voltages at motor terminals

The speed response under IT2FLC is illustrated in Fig. 13. As shown in the figure, the speed response is firstly set to a desired value of 3000 RPM, and then to a value of 2500 RPM during the period of (882–952) s. Lastly, a load of 0.2 N.m is applied during the period of (1090–1185) s. Compared with T1FLC, IT2FLC exhibits better tracking performance and load rejection capability. Table 2 quantifies the performance of both controllers in terms of their tracking and disturbance rejection capabilities. Performance is evaluated on the basis of the root mean square error (RMSE). The table shows that the RMSE values for IT2FLC is less than those for T1FLC in both tracking and robustness performance. Fig. 14 shows the torque trace developed by BLDCM throughout its operation.

Table-II: The performance of both controllers in terms of tracking

Control of Type	RMSE (at Speed Change)	RMSE (at Load Change)
Type-1 FL Controller	215.3040	208.3354
Interval Type-2 FL Controller	37.2126	39.0255

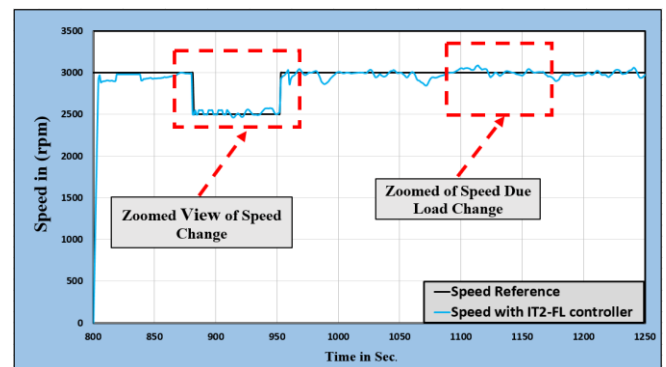


Fig. 13. The speed response of BLDC motor based on IT2FL controller

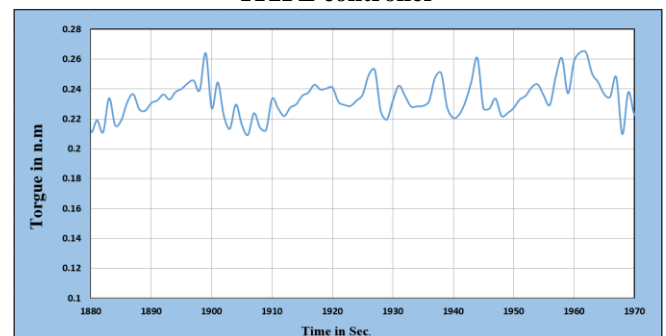


Fig. 14. The torque behavior developed by BLDC motor

VII. CONCLUSION

This article presents design and Implementation of speed control of BLDC motor based on two schemes of fuzzy logic control, represented by T1FL and IT2FL controllers. The design and implementation of FL-controlled speed control of BLDC motor is performed on the LabVIEW format. Within the environment of LabVIEW software, a performance comparison has been made between T1FL and IT2FL controllers in terms robustness characteristics. Based on the experimental results, The IT2FL controller shows that IT2FL controller shows better load rejection capability than T1FL controller.

REFERENCES

1. Arun Prasad K.M, Usha Nair, "An Intelligent Fuzzy Sliding Mode Controller for a BLDC Motor," *IEEE International Conference on Innovative Mechanisms for Industry Applications*, Volume 1, 2017, pp. 274-278.
2. Amjad J. Humaidi, Ibraheem Kasim Ibraheem, "Speed Control of Permanent Magnet DC Motor with Friction and Measurement Noise Using Novel Nonlinear Extended State Observer-Based Anti-Disturbance Control," *MDPI, Energies Journal*, 30 April 2019.
3. Amjad Jaleel Humaidi, Akram Hashim Hameed, "PMLSM position control based on continuous projection adaptive sliding mode controller," *Taylor & Francis, Systems Science & Control Engineering*, Volume 6, No. 3, pp.242–252, 2018.
4. Amjad J. Humaidi, Akram Hashim Hameed, Mustafa Riyadh Hameed, "Robust Adaptive Speed Control for DC Motor using Novel Weighted E-Modified MRAC," *IEEE International Conference on Power, Control, Signals and Instrumentation Engineering (ICPCSI)*, Chennai, India, p.p 313-319, 2017.
5. Amjad Jalil Humaidi, Akram Hashim Hameed, "Robustness enhancement of MRAC using modification techniques for speed control of three phase induction motor," *J. Electrical Systems*, Volume 13, pp. 723-741, 2017.
6. R. Arulmozhiyal, R. Kandiban, "Design of fuzzy PID controller for brushless DC motor," *In 2012 International Conference on Computer Communication and Informatics, IEEE*, 2012, pp. 1-7.
7. Blessy, MS Evangelin, and M. Murugan, "Modeling and controlling of BLDC motor based fuzzy logic," *In International Conference on Information Communication and Embedded Systems (ICICES2014)*, *IEEE*, 2014, pp. 1-6.
8. Shamseldin, et al., "Speed control of BLDC motor by using PID control and self-tuning fuzzy PID controller," *In 15th International Workshop on Research and Education in Mechatronics (REM)*, *IEEE*, 2014, pp. 1-9.
9. Krishnan, P. Hari, and M. Arjun "Control of BLDC motor based on adaptive fuzzy logic PID controller." *In 2014 International Conference on Green Computing Communication and Electrical Engineering (ICGCCEE)*, *IEEE*, 2014, pp. 1-5.
10. Akhila, M., and P. Ratnan, "Brushless DC motor drive with regenerative braking using adaptive neuro based fuzzy inference system," *In 2016 International Conference on Electrical, Electronics, and Optimization Techniques (ICEEOT)*, *IEEE*, 2016, pp. 748-751.
11. Xiong, et al., "Research on Speed Control System of Brushless DC Motor Based on Neural Network," *In 2015 8th International Conference on Intelligent Computation Technology and Automation (ICICTA)*, *IEEE*, 2015, pp. 761-764.
12. Muhammed A. Ibrahim, Ausama Kh. Mahmood and Nashwan Saleh Sultan, " Optimal PID controller of a brushless DC motor using genetic algorithm," *International Journal of Power Electronics and Drive System (IJPEDS)*, Vol. 10, No. 2, 2019, pp. 822-830.
13. N. N. Baharudin and S. M. Ayob. " Brushless DC Motor Speed Control Using Single Input Fuzzy PI Controller." *International Journal of Power Electronics and Drive System (IJPEDS)*, Vol. 9, No. 4, 2018, pp. 1952-1966.
14. Akhila, M., and P. Ratnan, "Brushless DC motor drive with regenerative braking using adaptive neuro based fuzzy inference system," *In 2016 International Conference on Electrical, Electronics, and Optimization Techniques (ICEEOT)*, *IEEE*, 2016, pp. 748-751.
15. Krishnan, Ramu, Permanent magnet synchronous and brushless DC motor drives. *CRC press*, 2009.

16. Hossein Rahimi Khoei, Elham Farazande Shahraki, "Fuzzy logic based direct power control of induction mot drive," *Bulletin of Electrical Engineering and Informatics*, Vol. 5, No. 3, 2016, pp. 296-306.
17. Ozek, Muzeyyen, Bulut, and Zuhtu Hakan Akpolat, "A software tool: Type-2 fuzzy logic toolbox," *Computer Applications in Engineering Education*, Vol. 16, no. 2, 2008, pp. 137-146.
18. Ying, Hao, Fuzzy control and modeling: analytical foundations and applications, *Wiley-IEEE Press*, 2000.
19. Passino, et al., Fuzzy control, Vol. 42. Menlo Park, CA: *Addison-wesley*, 1998.
20. Klir, George J., and Baozung Yuan, Fuzzy sets and fuzzy logic: theory and applications, Vol. 574. New Jersey: *Prentice Hall PTR*, 1995.
21. Ozek, et al., "A software tool: Type-2 fuzzy logic toolbox," *Computer Applications in Engineering Education*, Vol. 16, no. 2, 2008, pp. 137-146.
22. Mendel, et al., "Interval type-2 fuzzy logic systems made simple," *IEEE transactions on fuzzy systems*, Vol. 14, no. 6, 2006, pp. 808-821.

AUTHORS PROFILE



Hayder Yousif Abed: Was born in Baghdad, Iraq, in 1974. He received his B.Sc. in the College of Electrical Engineering from the University of Technology, Iraq, respectively in 2006. He received his M.Sc in 2012 from the University of Technology, Iraq. He is now a PhD student of University of Technology, Iraq. He research interests are power electronic.



Abdulrahim Thiab humod: Was born in Baghdad, Iraq, in 1961. He received his B.Sc. in the Department of Electrical and Electronic Engineering, Military engineering college, Iraq, respectively in 1984. He received his M.Sc in 1990 (control and guidance) from the Military engineering college, Iraq. His Ph.D. from Military engineering college (control and guidance) He is now a Asst. Professor in University of Technology, Iraq. He research interests are control and guidance.



Amjad J. Humaidi: He received his B.Sc. and M. Sc. degrees in Control engineering from Al-Rasheed College of Engineering and Science the University of Technology, Baghdad, Iraq, in 1992 and 1997, respectively. He received his Ph.D. degree from university of technology in 2006 with specialization of control and automation. He is presently deputy dean of control and system engineering department. His fields of interest include advanced control (adaptive control, backtepping control, nonlinear optimal control, nonlinear observers, and active rejection control), intelligent control, optimization and identification